

Design and application of high-sensitivity two-photon initiators for three-dimensional microfabrication

Stephen M. Kuebler^a, Kevin L. Braun^a, Wenhui Zhou^a, J. Kevin Cammack^{a,1}, Tianyue Yu^b, Christopher K. Ober^{b,*}, Seth R. Marder^{a,c,*}, Joseph W. Perry^{a,c,*}

^a Department of Chemistry, University of Arizona, Tucson, AZ 85721, USA

^b Department of Materials Science and Engineering, Cornell University, Ithaca, NY 14853, USA

^c Optical Sciences Center, University of Arizona, Tucson, AZ 85721, USA

Received 17 June 2002; accepted 1 July 2002

Abstract

A new photoacid generator (PAG) is described that can be efficiently activated by two-photon excitation (TPE) and can be used for high-sensitivity three-dimensional micro-patterning of acid-sensitive media. The molecule has a large two-photon absorption cross-section that peaks near 705 nm ($\delta = 690 \times 10^{-50} \text{ cm}^4 \text{ s photon}^{-1}$) and a high quantum yield for the photochemical generation of acid ($\phi_{\text{H}^+} \approx 0.5$). Under near-infrared laser irradiation, the molecule produces acid subsequent to TPE and initiates the polymerization of epoxides at an incident intensity that is one to two orders of magnitude lower than that needed for conventional ultraviolet-sensitive initiators. The new PAG was used in conjunction with the solid epoxide resist Epon SU-8 for negative-tone three-dimensional microfabrication and was incorporated into a chemically amplified resist for positive-tone fabrication of a three-dimensional microchannel structure.

© 2003 Elsevier Science B.V. All rights reserved.

Keywords: Two-photon absorption; Photoacid generator; Three-dimensional lithographic microfabrication; Positive-tone resist; Chemically amplified resist; Micro-electromechanical structures (MEMS); Microfluidics; Optical micro-electromechanical systems (OMEMS)

1. Introduction

Two-photon excitation (TPE) provides a means for activating chemical and physical processes with high spatial resolution in three dimensions using a single tightly focused laser beam. TPE has enabled the development of 3D fluorescence imaging [1], 3D lithographic microfabrication (3DLM) [2–7], and new approaches to 3D optical data storage [8,9]. Each of these applications takes advantage of the fact that the two-photon absorption (TPA) probability depends quadratically on the excitation intensity. By tightly focusing an excitation beam, the region of TPA can be confined at the focus to a volume of the order of the cube of the excitation wavelength ($V \sim \lambda^3$). Any subsequent process, such as fluorescence or a photo-induced chemical reaction, is also localized to this small volume.

Significant strides have been made in refining the 3DLM technique. The production of high-fidelity microstructures having complex 3D forms and features sizes as small as 100–200 nm has demonstrated the potential of this approach as a microfabrication tool [10–12]. Most work in the field has involved patterning structures in commercial acrylate resins using conventional ultra violet (UV)-active initiators [6,7,13]. Such initiators typically have low two-photon sensitivity, such that high excitation power and long exposure times are needed to cure the resin, which often result in damage to the structure. This aspect limits the versatility of 3DLM and its scope for widespread application. For 3DLM to become a commonly applied technique, high-sensitivity initiators are needed that make the process more reliable and allow structures to be patterned rapidly. New initiators are also needed so that the approach can be extended to other material systems based on chemistries other than free-radical polymerization. This will allow complex microstructures to be patterned in materials having physical and mechanical properties more suited to the target application.

We have reported a strategy for the design of organic molecules featuring large TPA cross-sections (δ) [14,15]. One structural motif for these molecules is D– π –D, where

* Corresponding authors.

E-mail addresses: jwperry@u.arizona.edu (J.W. Perry), cober@ccmr.cornell.edu (C.K. Ober), smarder@u.arizona.edu (S.R. Marder).

¹ Present address: Nitto Denko Technical Corporation, Oceanside, CA 92054, USA.

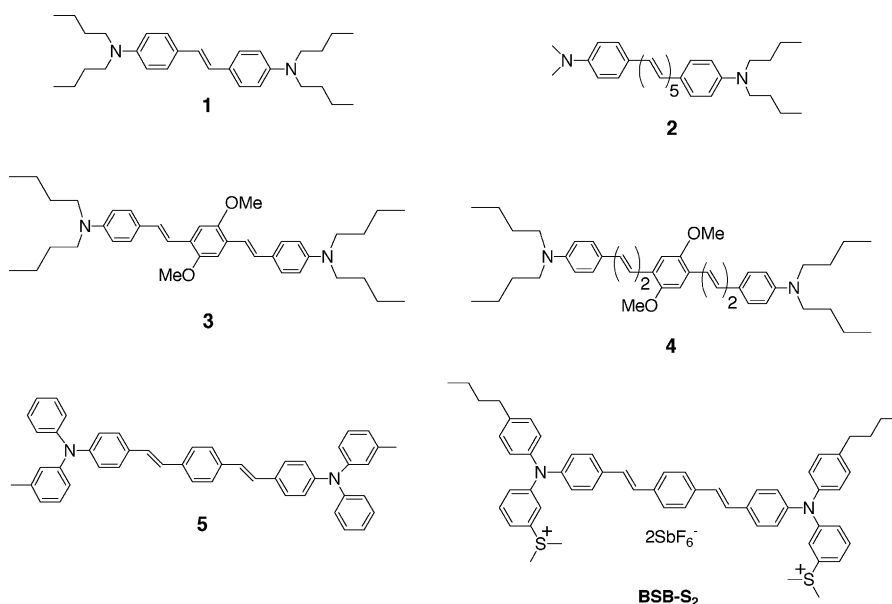


Fig. 1. (1–5) Examples of strongly two-photon-absorbing D– π –D chromophores. (BSB-S₂) Two-photon PAG discussed in this work.

π represents a π -conjugated backbone (for example, diphenylpolyene, *bis*(styryl)benzene, biphenyl), and D is an electron-donating group (for example, diphenylamino- or dibutylamino-) symmetrically substituted on the ends of the π -system. Examples of D– π –D molecules are given in Fig. 1. The maximum TPA cross-section of **1** was found to be $200 \times 10^{-50} \text{ cm}^4 \text{ s photon}^{-1}$ at 600 nm. The value of δ increases with conjugation length (1300×10^{-50} and $1420 \times 10^{-50} \text{ cm}^4 \text{ s photon}^{-1}$ for compounds **2** and **4**, respectively). Even larger values of δ have been measured for molecules with the generic structure D– π –A– π –D, in which electron withdrawing groups (A) are substituted on the central portion of the π -bridge [14]. These results have been interpreted in terms of a symmetric intramolecular electronic charge redistribution upon excitation that leads to large transition dipole moments between the electronic levels involved in the two-photon transition [14,15].

We have demonstrated that some of these D– π –D two-photon absorbers can be used as photoinitiators for the polymerization of acrylate monomers (for example, **1**, **3**, and **4**) [10,16]. The polymerization threshold pulse energy (or power for CW mode-locked excitation) for two-photon-induced polymerization (TPIP) using these chromophores was found to be substantially lower than that for conventional radical photoinitiators [10,17]. Experiments suggest that photoexcited D– π –D chromophores initiate the polymerization of acrylates through the generation of reactive species following transfer of an electron from the photoexcited D– π –D chromophore to an acrylate group. The improved efficiency of the D– π –D chromophores relative to conventional UV-sensitive initiators is associated with (1) the greatly increased TPA cross-section of the D– π –D molecule and (2) the ability of electron-rich D– π –D molecules to efficiently transfer charge to acrylate

acceptors. Complex 3D microstructures have been fabricated by 3DLM using these initiators [10,11,17].

In an effort to extend 3DLM to other material systems, we developed a new two-photon-activatable photoacid generator (PAG) [18]. PAGs are molecules that generate a Lewis or Brønsted acid (H^+) following photoexcitation [19]. PAGs can be used to photoinitiate the cationic polymerization of epoxides and vinyl ethers [20]. Epoxide resins containing a PAG are routinely used for two-dimensional lithographic patterning [21,22]. Conventional UV-sensitive PAGs, such as diaryliodonium and triarylsulfonium cations, have been used for two-photon microfabrication [23]. However, the TPA cross-sections of these initiators are typically very small ($\delta \sim 10 \times 10^{-50} \text{ cm}^4 \text{ s photon}^{-1}$), and as a result they exhibit low two-photon sensitivity. Previously, we proposed that the design of highly photosensitive two-photon initiators requires: (1) a chromophoric group with a large δ ; (2) a functionality that can generate an initiating species with high efficiency; and (3) a mechanism through which excitation of the chromophore leads efficiently to activation of the chemical functionality [10]. Following this principle, we developed the two-photon-activatable PAG **BSB-S₂**, shown in Fig. 1. **BSB-S₂** consists of a *bis*[(diarylamino)styryl]benzene core with covalently attached sulfonium moieties. The *bis*[(diarylamino)styryl]benzene fragment is a D– π –D structure, like that of **5**, which possesses a high TPA cross-section ($\delta = 805 \times 10^{-50} \text{ cm}^4 \text{ s photon}^{-1}$) peaking in the near infrared ($\lambda_{\text{max}}^{(2)} = 745 \text{ nm}$) [15]. The dialkylaryl-sulfonium group is known to efficiently generate H^+ when reduced by a one-electron transfer process [24,25]. From the electrochemical and spectroscopic measurements of Saeva [26,27] and our own studies [14,15], we determined that the D– π –D core is sufficiently electron-rich and the first electronic excited-state (populated by either one- or two-photon

excitation) is sufficiently energetic that the photoexcited D- π -D core should efficiently transfer an electron to the sulfonium group leading to H⁺ generation. Consequently, **BSB-S₂** is designed to have the features needed for it to be an efficient one- and two-photon-activatable PAG. In this work, we provide evidence that **BSB-S₂** is an efficient two-photon PAG and we demonstrate its use for high-sensitivity 3DLM in an epoxide resin and a positive-tone chemically amplified resist.

2. Experimental

2.1. Synthesis of **BSB-S₂**

The *bis*[(diarylamino)styryl]benzene functionalized with sulfonium groups (**BSB-S₂**) was prepared from 3-bromothiophenol in seven steps (Fig. 2). Alkylation of sodium 3-bromothiophenoxide with methyl iodide in methanol produced 3-bromophenyl methyl sulfide in a yield of 86%. Pd-catalyzed coupling of 3-bromophenyl methyl sulfide with 4-butylaniline following the method of Driver and Hartwig [28] gave sulfur-containing secondary amine **6** in a yield of 78%. Again Pd-catalyzed coupling of **6** with dioxalane-protected 4-bromo-benzaldehyde, followed by acid-deprotection of the dioxalane gave 4-*n*-butyl-4'-formyl-3''-methylthio triphenylamine (**8**) in a yield of 79% for the two steps. **8** reacted with tetraethyl α,α' -*p*-xylylenebisphosphonate under standard Horner–Emmons conditions to yield the sulfide precursor, *E,E*-1,4-bis[4-(*N*-4-*n*-butylphenyl)-*N*-3-{methyl-thio}-phenyl]aminostyryl]benzene (**9**) in 95%. Alkylation of **9** with methyl trifluoromethanesulfonate employing a modified method of Saeva and Morgan [29] gave the triphenylamine sulfonium triflate salt. Non-nucleophilic anions, such as SbF₆⁻, which are required for cationic polymerization, were exchanged by repeating a metathesis reaction

three times using an excess of the sodium salt of the anion. These compounds were characterized by multinuclear NMR and elemental analysis.

2.2. Measurement of the quantum yield for photogeneration of acid

Solutions of **BSB-S₂** in acetonitrile (4.0×10^{-4} M) were irradiated at 400 nm using either a Xenon lamp or a frequency-doubled mode-locked Ti:sapphire laser. At this concentration more than 99% of the light was absorbed. The photogenerated acid, H⁺, was titrated by the addition of excess rhodamine B base in acetonitrile (6.0×10^{-5} M after addition) and quantified spectrophotometrically from the absorbance of protonated rhodamine B base [30]. The acid-yield increased linearly with both the excitation intensity and time, consistent with acid generation being initiated by one-photon excitation. The ratio of photogenerated H⁺ to the number of photons absorbed gave the quantum yield for the photogeneration of acid, ϕ_{H^+} .

2.3. Two-photon-excitation and two-photon acid-yield action spectra

TPE and two-photon acid-yield action spectra were recorded using 4.0×10^{-4} M solutions of **BSB-S₂** in acetonitrile irradiated in 1 cm path-length fluorescence cells using focused ($f = 75$ mm) 80 fs pulses from a CW mode-locked Ti:sapphire laser (82 MHz, 8.5 mm diameter spot-size at lens). The TPE spectrum was recorded using the two-photon-fluorescence method [14,31], with fluorescein in water (1.54×10^{-5} M, pH = 11) as a reference. The up-converted fluorescence was detected at 520 nm and its intensity was found to be proportional to the square of the excitation power, as expected for TPA. The concentration of the photogenerated acid, [H⁺], was determined

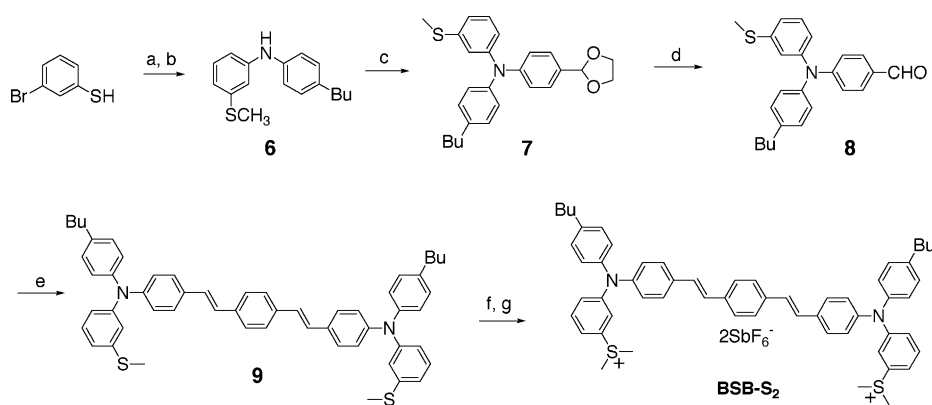


Fig. 2. Scheme for the synthesis of **BSB-S₂**: (a) methyl iodide, sodium methoxide, methanol, 86%; (b) 1,1'-*bis*[(diphenylphosphino)ferrocene] (DPPF), *tris*-(dibenzylideneacetone)dipalladium(0) (Pd₂(dba)₃), 4-*n*-butylaniline, sodium *tert*-butoxide, toluene, 90 °C, 78%; (c) 1,4-bromo-(1,3-dioxolan-2-yl)benzene, Pd₂(dba)₃, DPPF, sodium *tert*-butoxide, toluene, 90 °C; (d) HCl, tetrahydrofuran, 79% for (c) and (d); (e) tetraethyl α,α' -*p*-xylylenebisphosphonate, potassium *tert*-butoxide, tetrahydrofuran, 0 °C, 95%; (f) methyl trifluoromethanesulfonate, dichloromethane; (g) sodium hexafluoroantimonate, acetone, water (62% for (f) and (g)).

spectrophotometrically following a 30 min exposure at each TPE wavelength. The two-photon acid-yield action spectrum was constructed by dividing $[H^+]$ by the ratio of the emission counts and the TPE action cross-section of the fluorescein reference ($(F(t)/\phi_f\delta)_{\text{ref}}$ (to account for the temporal and spatial dependence of the excitation intensity as a function of wavelength) [31] and normalizing to δ of **BSB-S₂** at 705 nm. For both experiments, the concentration of **BSB-S₂** decreased by less than 2.5% after exposure.

2.4. Dose-array measurement of the two-photon-induced epoxide polymerization threshold using nanosecond laser pulses

A cell was fashioned by sandwiching a 2 mm thick o-ring between two glass substrates, one of which was treated with a trimethoxy[2-(7-oxabicyclo[4.1.0]hept-3-yl)ethyl]silane adhesion promoter. The cell was filled with 10 mM **BSB-S₂** in 20/80% Epon SU-8 (Shell)/4-vinyl-1-cyclohexene diepoxide (1.3 wt.% PAG). An array of points in the cell was irradiated with focused 5 ns laser pulses at a wavelength of 745 nm (10 Hz repetition rate; 500 mm focal length lens; 5 mm beam diameter at the lens) to determine the threshold pulse energy for the onset of polymerization under different exposure times. Along one axis of the array, the pulse energy was varied from 0.8 to 4.5 mJ. Along the other axis, the exposure time was varied from 1 to 20 s. At an irradiation spot, the onset of polymerization was marked by the appearance of a ringed diffraction pattern in the far-field transmitted beam. For a given exposure time, the polymerization threshold pulse energy was taken as the average of the lowest and highest pulse energies for which polymerization was observed and not observed, respectively. Extensive cross-linking ultimately resulted in disruption of the far-field pattern and formation of a column of cross-linked polymer that spanned the length of the cell in the irradiated region. Following exposure, the cell was disassembled and rinsed with propylene glycol methylether acetate. Free-standing columns of two-photon cross-linked polymer remained on the adhesion-promoted substrate.

2.5. Measurement of the epoxide polymerization threshold under CW mode-locked near-infrared laser excitation

Test resins of each of a given set of initiators (10 mM) in Araldite CY179MA (Ciba, 7-oxabicyclo[4.1.0]heptane-3-carboxylic acid, 7-oxabicyclo[4.1.0]hept-3-ylmethyl ester) were irradiated with focused ($f = 75$ mm) 80 fs pulses from a Ti:sapphire laser (82 MHz repetition rate, 0.94 mm diameter spot-size at lens). The threshold power for the onset of polymerization within a 10 s exposure at a given irradiation wavelength was established by the advent of a circular diffraction pattern in the far-field of the transmitted beam. Under conditions for which polymerization was observed, exposure at higher powers and for longer times produced clearly visible solid features of cross-linked polymer.

2.6. Microfabrication using a **BSB-S₂**/epoxide resin

In the dark, 393 mg of SU-8, 262 mg of γ -butyrolactone, and 10.2 mg of **BSB-S₂** (2.5 wt.% in resin) were stirred until the solids had dissolved. The resin mixture was blade-casted onto a substrate treated with a trimethoxy[2-(7-oxabicyclo[4.1.0]hept-3-yl)ethyl]silane adhesion promoter at a thickness of 510 μm , dried in air at room temperature for 10 days, then heated on a hot-plate at 100 °C for 15 min. The resulting solid film had a thickness of 330 ± 100 μm . The film was exposed in a target three-dimensional pattern by tightly focusing 80 fs pulses from a Ti:sapphire laser at a wavelength of 745 nm into the resin while translating the focal point at a speed of 50 $\mu\text{m/s}$ ($60 \times /1.4$ NA oil-immersion objective, 82 MHz pulse repetition rate) [10,11]. The average optical power at the film was varied between 1 and 5 mW. Following irradiation, the film was immersed in γ -butyrolactone for 60 min to remove the unexposed resin, and then rinsed with methanol, leaving the cross-linked epoxide microstructure standing freely on the substrate.

2.7. Microfabrication using a positive-tone chemically amplified resist containing **BSB-S₂**

A 50 μm thick film of 1 wt.% **BSB-S₂** in tetrahydropyranyl methacrylate (THPMA)–methyl methacrylate (MMA)–methacrylic acid (MA) (see below) was exposed in the pattern of a target structure at 745 nm with tightly focused (1.4 NA) 80 fs pulses from a Ti:sapphire laser (82 MHz repetition rate) at an average power of 500 μW and a linear scan speed of 50 $\mu\text{m/s}$. After irradiation, the film was baked for 1 min at 90 °C. The final structure was then obtained by dissolving the exposed resin in aqueous 0.26 M tetramethylammonium hydroxide.

3. Results and discussion

The one-photon absorption (UV-visible) and TPE spectra for solutions of **BSB-S₂** in acetonitrile are shown in Fig. 3A. The lowest energy absorption in the UV-visible spectrum has a maximum at $\lambda_{\text{max}} = 392$ nm ($\epsilon_{392} = 5.5 \times 10^4 \text{ M}^{-1} \text{ cm}^{-1}$). The TPE spectrum shows that **BSB-S₂** exhibits strong TPA from 705 to 850 nm ($\delta > 100 \times 10^{-50} \text{ cm}^4 \text{ s photon}^{-1}$) that peaks near 705 nm ($\delta = 690 \times 10^{-50} \text{ cm}^4 \text{ s photon}^{-1}$). Together these spectra indicate that the lowest energy electronic excited state, S_1 , is populated by one-photon excitation and lies at an energy of 3.17 eV above the ground state. The next electronic excited state, S_2 , lies at slightly higher energy than S_1 , near 3.52 eV relative to the ground state. These features are consistent with measurements obtained for similar *bis*[(diarylamino)styryl]benzenes [15]. For the model unsubstituted *bis*[(diarylamino)styryl]benzene **5** (lacking sulfonium groups), S_1 and S_2 lie at energies of 3.02 and

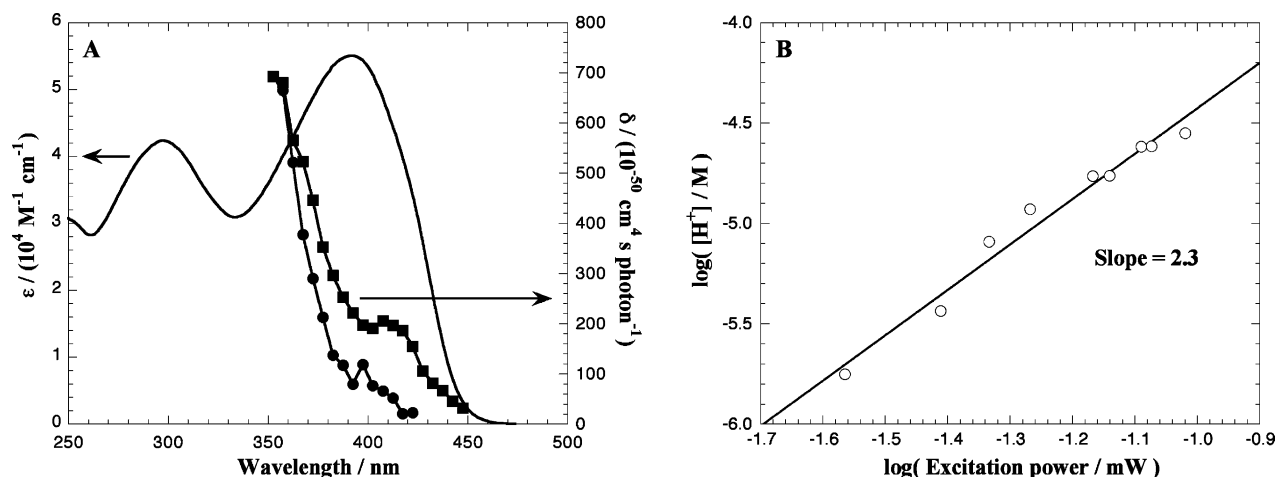


Fig. 3. (A) One-photon absorption spectrum (solid line), TPE spectrum (■), and two-photon acid-yield action spectrum (●) of **BSB-S₂** in acetonitrile. The TPE and acid-yield spectra are plotted versus half of the excitation wavelength. The one-photon absorption spectrum was recorded using a 2.2×10^{-5} M solution. (B) Plot of $\log([H^+])$ against $\log[\text{excitation power/mW}]$ at 745 nm. The smooth curve is the best fit of a line to the data and has a slope of 2.3, which indicates that the acid-yield increases quadratically with the excitation intensity.

3.33, respectively (in toluene). Studies of donor-substituted π -conjugated systems would suggest that S_1 and S_2 should shift to higher energy as the electron-donating strength of the donor-groups decreases [32]. Thus, the shift of S_1 and S_2 for **BSB-S₂** to higher energy relative to **5** is most likely caused by the electron-poor sulfonium groups weakening the donor strength of the diarylamino groups.

From studies of other organic chromophores [33], and other D- π -D chromophores specifically [15], one expects that the population created in S_2 following TPE will rapidly transfer to S_1 by internal conversion. S_1 then depopulates by fluorescence or non-radiative processes. The close proximity of the electron-accepting sulfonium group is expected to result in efficient excited-state electron-transfer, accompanied by acid generation and quenched fluorescence emission from S_1 . Solutions of **BSB-S₂** in acetonitrile become acidic following one- and two-photon irradiation and are weakly fluorescent. The fluorescence quantum efficiency under one-photon excitation was measured to be $\phi_f = 0.013 \pm 0.001$ (in acetonitrile), which is much lower than that of unsubstituted **5** ($\phi_f = 0.93$ in toluene) [15]. The quantum efficiency for proton generation under one-photon excitation is $\phi_{H^+} = 0.50 \pm 0.05$. This value is comparable to or greater than most commercial UV-sensitive PAGs [34]. It is also consistent with the excited state of the *bis*[(diarylamino)styryl]benzene core being quenched efficiently by transfer of an electron to the dimethylsulfonium group. Measurements of the acid generated under TPE at 745 nm show that the acid-yield increases with the square of the excitation intensity (Fig. 3B). Additionally, the two-photon acid-yield action spectrum qualitatively follows the TPE spectrum (Fig. 3A). These data demonstrate that **BSB-S₂** efficiently generates acid when excited by TPA. The two-photon acid-generation efficiency can be quantified by the figure of merit $\delta\phi_{H^+} \approx 350 \times 10^{-50} \text{ cm}^4 \text{ s photon}^{-1}$ (at 705 nm).

The acid photogenerated by **BSB-S₂** was found to initiate the polymerization of a wide range of epoxides, including cyclohexene oxide, 4-vinyl-cyclohexene dioxide, Araldite CY179MA, and the cross-linkable solid epoxide SU-8. For example, irradiating an 8×10^{-7} M solution of **BSB-S₂** in 80% (by volume) cyclohexene oxide in dichloromethane at 419 nm yielded polymer that precipitated following the addition of methanol. **BSB-S₂** also proved to be a high-sensitivity initiator for cationic polymerization of various epoxide monomers under diverse TPE conditions utilizing nanosecond or femtosecond laser pulses. Fig. 4 shows a scanning electron microscope (SEM) image of columnar structures produced with nanosecond laser pulses at 745 nm

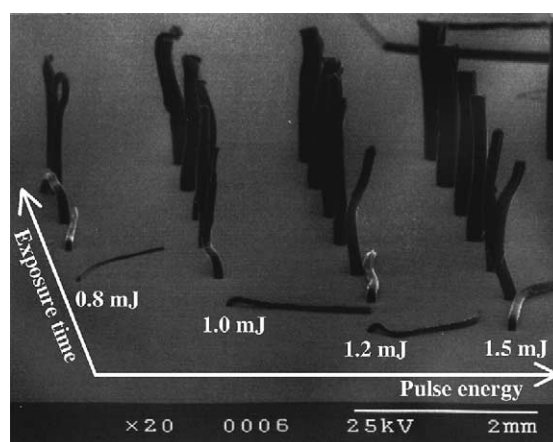


Fig. 4. SEM image of some of the columnar structures produced by irradiating 10 mM **BSB-S₂** in 20/80% SU-8/4-vinyl-1-cyclohexene diepoxide with 5 ns laser pulses at 745 nm during a dose-array measurement of the TPIP threshold. The width of the smallest feature is 60 μm . Across the array, the pulse energy increases from left to right, and the exposure time increases from front to back. For the four columns visible, the pulse energies used are 0.8, 1.0, 1.2, and 1.5 mJ.

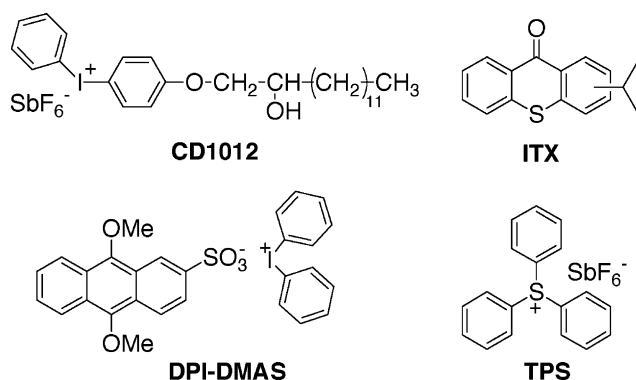


Fig. 5. Structures of some conventional PAGs. CD1012 = [4-[(2-hydroxytetradecyl)oxy]phenyl]phenyliodonium hexafluoroantimonate, ITX = isopropylthioxanthone, DPI-DMAS = diphenyliodonium 9,10-dimethoxyanthracene sulfonate, TPS = triphenylsulfonium hexafluoroantimonate.

during a dose-array measurement of the TPIP threshold for 10 mM **BSB-S₂** in 20/80% SU-8/4-vinyl-1-cyclohexene diepoxide. The polymerization threshold energies were found to be 2.1, 1.4, 0.9, and 0.9 mJ for exposure times of 1, 2, 3, and 5 s, respectively. Columns were also generated using similar conditions in **BSB-S₂**-containing resins of 20/80% SU-8/cyclohexene oxide, neat Araldite CY179MA, and solid films of SU-8.

There are few reports of two-photon-initiated cationic polymerization of epoxides [23,35], and each of these involves the use of UV-sensitive PAGs that have very low two-photon sensitivity. We compared the epoxide polymerization sensitivity of **BSB-S₂** under near-infrared CW mode-locked laser excitation with that of four widely used PAGs (Fig. 5): CD1012 (Sartomer), CD1012/ITX (1:1.6 molar ratio), TPS, and DPI-DMAS. The threshold power for the onset of polymerization was determined for resins containing each initiator when irradiated at 710 and 760 nm. The 710 nm excitation was used to duplicate the conditions employed in previous studies of CD1012/ITX (1:1.6 molar ratio) [35], and because this wavelength is near the TPA peak of **BSB-S₂**. The 760 nm excitation was also used as

Table 1

Polymerization threshold powers (mW) for Araldite CY179MA epoxide resins containing the indicated initiator under CW mode-locked laser excitation at 710 and 760 nm

| Initiator | 710 nm | 760 nm |
|--------------------------|-------------------|-------------------|
| BSB-S₂ | 2.4 | 5.6 |
| CD1012/ITX | 44 | 50 |
| CD1012 | 212 | 560 |
| TPS | >317 ^a | >655 ^a |
| DPI-DMAS | >317 ^a | 468 |

^a No polymerization was observed at the maximum available power.

this closely matches the conditions employed in earlier studies of CD1012 [23] and should be the optimum two-photon wavelength for activating DPI-DMAS [36]. The measured polymerization threshold powers are summarized in Table 1. Similar threshold powers were found for resins based on 4-vinyl-cyclohexene dioxide. The data demonstrate that the two-photon sensitivity of **BSB-S₂** is nearly one order of magnitude greater than that of the best-performing conventional initiator (CD1012/ITX), and more than two orders of magnitude greater than that of TPS, a commercial initiator commonly used in industry. This dramatic increase in two-photon-sensitivity results because **BSB-S₂** has been designed to include: (1) a strongly two-photon-absorbing chromophore and (2) a chemical functionality that efficiently generates [H⁺] following electronic excitation of the chromophore.

The technology of 3DLM is promising in that complex 3D microstructures, that would be either difficult or time-consuming to fabricate by any other approach, can be produced in a single exposure step [4,5,10,11,17,37–39]. We experienced limited success in attempts to microfabricate 3D structures in thick films of SU-8 containing conventional PAGs, like those of Fig. 5, using near-infrared excitation. High exposure powers (>8 mW) were needed to achieve suitable cross-linking with these low-sensitivity initiators, and typically the material was damaged during the patterning. In contrast, we could reliably fabricate complex 3D structures in films of SU-8 containing **BSB-S₂** as the two-photon PAG. Fig. 6 shows a series of structures that were

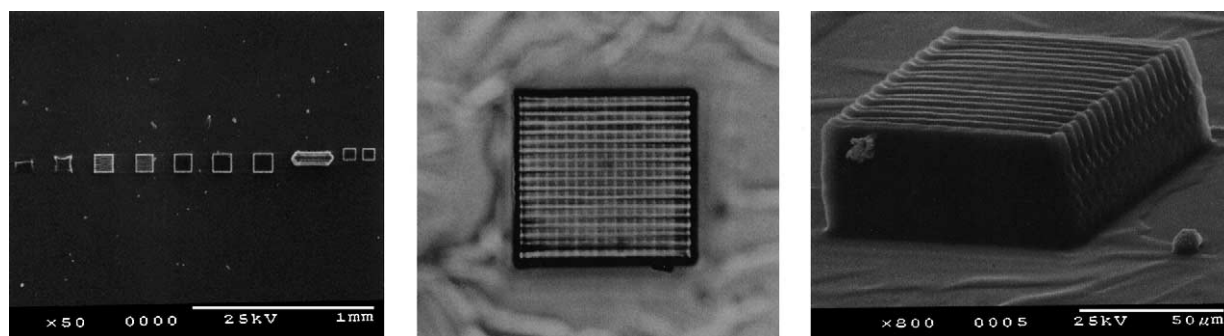


Fig. 6. Images of microstructures created by patterned two-photon irradiation of an epoxide resin containing **BSB-S₂**. (Left) SEM image of microstructures created with average exposure powers of 1–5 mW; (center) optical transmission micrograph of a “stack-of-logs” photonic bandgap structure fabricated with an average power of 3.5 mW; (right) SEM image of the microstructure shown in the center.

produced using exposure powers of 1–5 mW. Previously, we demonstrated that a wide range of microstructures—having possible applications in the areas of MEMS, microfluidics, and microoptical systems—could be generated using high two-photon-sensitivity acrylate resins based on D- π -D initiators. The present work demonstrates that high-fidelity microfabrication is now possible in epoxide resins using **BSB-S₂** as the two-photon PAG. Reliable 3DLM using **BSB-S₂** is possible because the high-two-photon sensitivity of the PAG allows exposure powers below the material damage threshold to be used during patterning.

The epoxide-based resins are “negative-tone” systems, in which the exposed regions of the resin become insoluble in a post-exposure development solvent. The polymer structure is then a replica of the exposure pattern. In contrast, positive-tone resists are solid-state systems for which the exposed regions become soluble in a developer. The final structure is then the complement of the exposure pattern. The use of a positive-tone resist in 3D microfabrication is desirable for a number of applications. For example, it should be simpler and more efficient to construct microfluidic devices by excavating material, rather than building up the walls of each microchannel in the structure using a negative-tone resist. In addition, positive-tone resists should help minimize the shrinkage and distortion typically encountered in

the photoprocessing of acrylates and other negative-tone resists.

We have developed a solid-state acid-sensitive positive-tone chemically amplified resist, designed for 3DLM using **BSB-S₂** as the two-photon PAG. The resist (Fig. 7A) is a random co-polymer of THPMA, MMA, and MA. In the presence of photogenerated acid, an ester-cleavage reaction converts the THP-ester-groups to carboxylic acid groups and renders the exposed material soluble in aqueous base developer. To illustrate the use of **BSB-S₂**/THPMA–MMA–MA for positive-tone microfabrication, we exposed a thick film of the resist in the pattern of the microchannel structure depicted schematically in Fig. 7B using an average power of 500 μ W. The target structure consists of two prism-shaped cavities (top: 43 μ m \times 32 μ m) extending from the surface of the film to a depth of 23 μ m. The cavities are connected by two channels lying 13 μ m below the surface and having a cross-section size of 4 μ m \times 5 μ m. After irradiating the film and removing the exposed material, two-photon-fluorescence image-slices (Fig. 7C–E) were recorded at three depths from the surface. The images reveal that the channels make a continuous connection between the cavities and are submerged below the surface of the film. An SEM image of the structure (Fig. 7F) shows that the channels lie below the film surface and are open

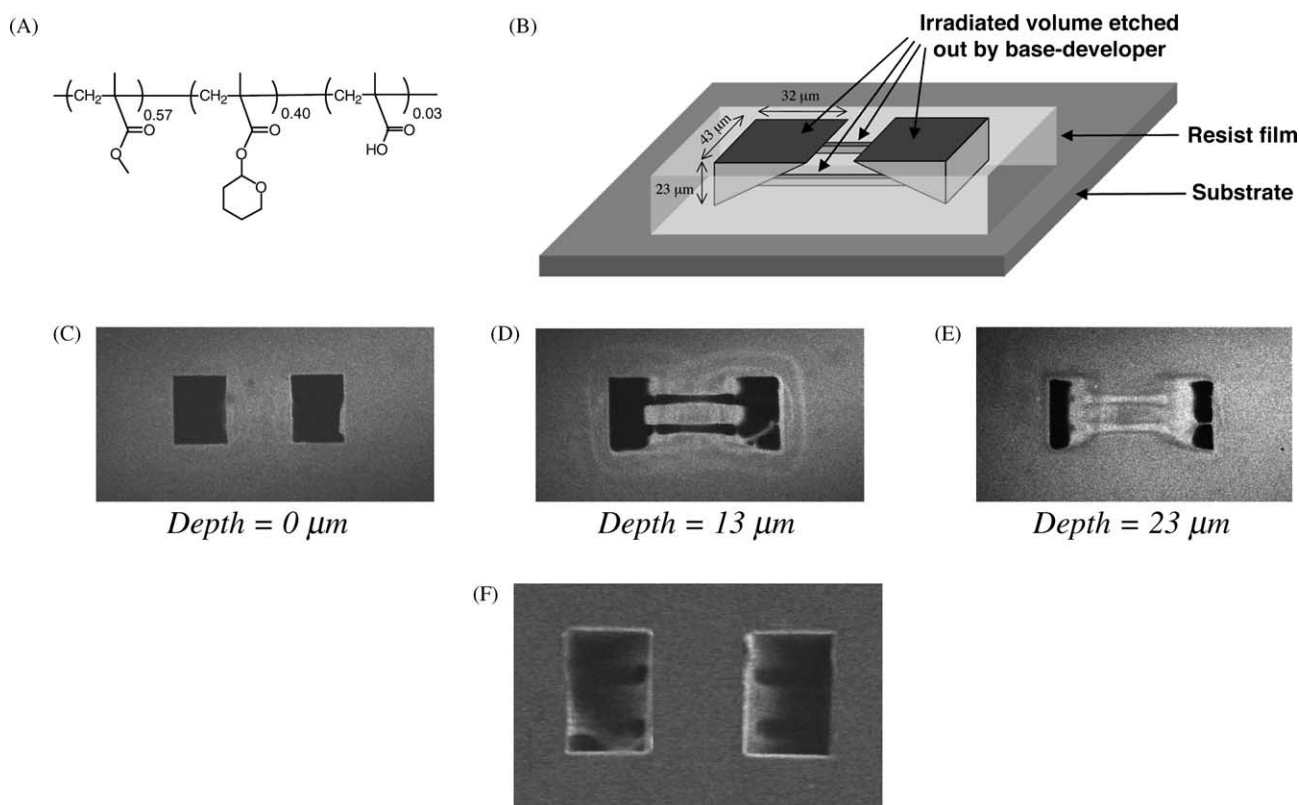


Fig. 7. (A) Structure of the THPMA–MMA–MA chemically amplified resist. (B) Schematic illustration of the target microstructure consisting of two prism-shaped cavities (width: 32 μ m, length: 43 μ m, depth: 23 μ m), that are connected by 2 channels (4 μ m by 5 μ m cross-section) lying 13 μ m below the surface. (C–E) Two-photon-fluorescence image-slices of the final structure (viewed normal to the substrate): (C) at the surface of the film; (D) 13 μ m below the surface; (E) 23 μ m below the surface. (F) SEM image of the final structure.

to the cavities, that extend to the film surface at either end. We found that the channels can be back-filled with liquids, including liquid crystals. This demonstration illustrates that the **BSB-S₂/THPMA–MMA–MA** material system can be used to pattern complex 3D structures, and suggests that microfluidic structures and even microoptical structures—such as gratings, waveguides, and photonic lattices—can be fabricated readily. The low irradiation power used to pattern the structure also demonstrates the high two-photon-sensitivity of this new microfabrication material system.

4. Conclusions

We have designed and synthesized a new two-photon PAG, that offers as much as two orders of magnitude improved sensitivity relative to conventional PAGs. The application of this two-photon PAG has been illustrated with 3D microfabrication using a negative-tone cross-linkable epoxide resin and a chemically amplified positive-tone resist. These material systems should be of use for the fabrication of MEMS structures. The positive-tone resists can be of particular use in microfluidics application and as templates for the production of various complex microoptical elements. The approach outlined and demonstrated here for the synthesis of the PAG should be applicable to the design of other high-sensitivity two-photon initiators, including two-photon radical and base generators. The advent of high-sensitivity initiators for two-photon patterning of radical- and acid-activated material should allow 3DLM to become more widely applied.

Acknowledgements

Support from the Air Force Office of Scientific Research (#F49620-99-1-0019 and #F49620-97-1-0014), the National Science Foundation (#CHE-0107105 and #DMR-9975961), the Office of Naval Research (#N00014-95-1319 and #N000141-01-1-0633), the NSF-funded Cornell Nanobiotechnology Center, and the Defense University Research Instrumentation Program (#N00014-99-1-0541 and #F49620-00-1-0161) is gratefully acknowledged. We wish to thank Dr. Mariacristina Rumi for many useful discussions.

References

- [1] W. Denk, Proc. Natl. Acad. Sci. 91 (1994) 6629.
- [2] W. Denk, J.H. Strickler, W.W. Webb, Science 248 (1990) 73.
- [3] J.H. Strickler, W.W. Webb, Opt. Lett. 16 (1991) 1780.
- [4] J.H. Strickler, W.W. Webb, Proc. Soc. Photo-opt. Instrum. Eng. 1398 (1990) 107.
- [5] E.S. Wu, J.H. Strickler, W.R. Harrell, W.W. Webb, Proc. Soc. Photo-opt. Instrum. Eng. 1674 (1992) 776.
- [6] S. Maruo, O. Nakamura, S. Kawata, Opt. Lett. 22 (1997) 132.
- [7] S. Maruo, S. Kawata, J. Microelectromech. Syst. 7 (1998) 411.
- [8] D.A. Parthenopoulos, P.M. Rentzepis, Science 245 (1989) 843.
- [9] H.E. Pudavar, M.P. Joshi, P.N. Prasad, B.A. Reinhardt, Appl. Phys. Lett. 74 (1999) 1338.
- [10] B.H. Cumpston, S.P. Ananthavel, S. Barlow, D.L. Dyer, J.E. Ehrlich, L.L. Erskine, A.A. Heikal, S.M. Kuebler, I.-Y.S. Lee, D. McCord-Maughon, J. Qin, H.R. Röckel, M. Rumi, X.-L. Wu, S.R. Marder, J.W. Perry, Nature 398 (1999) 51.
- [11] S.M. Kuebler, M. Rumi, T. Watanabe, K. Braun, B.H. Cumpston, A.A. Heikal, L.L. Erskine, S. Thayumanavan, S. Barlow, S.R. Marder, J.W. Perry, J. Photopolym. Sci. Technol. 14 (2001) 657.
- [12] S. Kawata, H.-B. Sun, T. Tanaka, K. Takada, Nature 412 (2001) 697.
- [13] K.D. Belfield, X. Ren, E.W. van Stryland, D.J. Hagan, V. Dubikovskiy, E.J. Miesak, J. Am. Chem. Soc. 122 (2000) 1217.
- [14] M. Albota, D. Beljonne, J.-L. Brédas, J.E. Ehrlich, J.-Y. Fu, A.A. Heikal, S.E. Hess, T. Kogej, M.D. Levin, S.R. Marder, D. McCord-Maughon, J.W. Perry, H. Röckel, M. Rumi, G. Subramaniam, W.W. Webb, X.-L. Wu, C. Xu, Science 281 (1998) 1653.
- [15] M. Rumi, J.E. Ehrlich, A.A. Heikal, J.W. Perry, S. Barlow, Z. Hu, D. McCord-Maughon, T.C. Parker, H. Röckel, S. Thayumanavan, S.R. Marder, D. Beljonne, J.-L. Brédas, J. Am. Chem. Soc. 122 (2000) 9500.
- [16] B.H. Cumpston, J.E. Ehrlich, L.L. Erskine, A.A. Heikal, Z.-Y. Hu, I.-Y.S. Lee, M.D. Levin, S.R. Marder, D.J. McCord, J.W. Perry, H. Röckel, M. Rumi, X.-L. Wu, in: J.R. Reynolds, A.K.-Y. Jen, M.F. Rubner, L.Y. Chiang, L.R. Dalton (Eds.), Proceedings of the Symposium on Electrical, Optical, and Magnetic Properties of Organic Solid-state Materials IV, vol. 488, Material Research Society, Warrendale, 1998.
- [17] S.M. Kuebler, B.H. Cumpston, S. Ananthavel, S. Barlow, J.E. Ehrlich, L.L. Erskine, A.A. Heikal, D. McCord-Maughon, J. Qin, H. Röckel, M. Rumi, S.R. Marder, J.W. Perry, Micro- and Nano-photonics Materials and Devices, San Jose, CA, Soc. Photo-opt. Instrum. Eng. 3937 (2000) 97.
- [18] W. Zhou, S.M. Kuebler, K.L. Braun, T. Yu, J.K. Cammack, C.K. Ober, J.W. Perry, S.R. Marder, Science 296 (2002) 1106.
- [19] C. Roffey, Photogeneration of Reactive Species for UV Curing, Wiley, New York, 1997.
- [20] G. Odian, Principles of Polymerization, 2nd ed., Wiley, New York, 1981.
- [21] C.G. Willson, H. Ito, J.M.J. Fréchet, T.G. Tessier, F.M. Houlihan, J. Electrochem. Soc. 133 (1986) 181.
- [22] J.M.J. Fréchet, F. Bouchard, F.M. Houlihan, B. Kryczka, E. Eichler, N. Clecak, C.G. Willson, J. Imag. Sci. 30 (1986) 59.
- [23] K.D. Belfield, K.J. Schafer, Y.U. Liu, J. Liu, X.B. Ren, E.W. van Stryland, J. Phys. Org. Chem. 13 (2000) 837.
- [24] R.W. Angelo, J.D. Gelorme, J.P. Kuczynski, W.H. Lawrence, S.P. Pappas, L.L. Simpson, US Patent 5,047,568 (1991).
- [25] R.W. Angelo, J.D. Gelorme, J.P. Kuczynski, W.H. Lawrence, S.P. Pappas, L.L. Simpson, US Patent 5,102,772 (1992).
- [26] F.D. Saeva, Adv. Electr. Trans. Chem. 4 (1994) 1.
- [27] F.D. Saeva, D.T. Breslin, P.A. Martic, J. Am. Chem. Soc. 111 (1989) 1328.
- [28] M.S. Driver, J.F.J. Hartwig, J. Am. Chem. Soc. 118 (1996) 7217.
- [29] F.D. Saeva, B.P. Morgan, J. Am. Chem. Soc. 106 (1984) 4121.
- [30] G. Pohlers, J.C. Scaiano, R. Sinta, Chem. Mater. 9 (1997) 3222.
- [31] C. Xu, W.W. Webb, J. Opt. Soc. Am. B 13 (1996) 481.
- [32] J. Cornil, D.A. dos Santos, D. Beljonne, J.L. Brédas, J. Phys. Chem. 99 (1995) 5604.
- [33] C.A. Parker, Photoluminescence of Solutions, Elsevier, Amsterdam, 1968.
- [34] M. Shirai, M. Tsunooka, Prog. Polym. Sci. 21 (1996) 1.
- [35] Y. Boiko, J.M. Costa, M. Wang, S. Esener, Opt. Express 8 (2001) 571.
- [36] K. Naitoh, T. Yamaoka, A. Umehara, Chem. Lett. (1991) 1869.
- [37] G. Witzgall, R. Vrijen, E. Yablonovitch, V. Doan, B.J. Schwartz, Opt. Lett. 23 (1998) 1745.
- [38] H.-B. Sun, T. Kawakami, Y. Xu, J.-Y. Ye, S. Matuso, H. Misawa, M. Miwa, R. Kaneko, Opt. Lett. 25 (2000) 1110.
- [39] S. Maruo, K. Ikuta, Proc. Soc. Photo-opt. Instrum. Eng. 3937 (2000) 106.